J Fluoresc (2012) 22:475–483
DOI 10.1007/s10895-011-0981-5

ORIGINAL PAPER

Cool White Light Emission in Dysprosium and Salicylic Acid Doped Poly Vinyl Alcohol Film Under UV Excitation

Gagandeep Kaur · S. B. Rai

Received: 24 August 2011 / Accepted: 13 September 2011 / Published online: 27 September 2011

Abstract Dysprosium (Dy) and Salicylic acid (Sal) doped Poly Vinyl Alcohol (PVA) films have been successfully prepared by solution cast technique. The absorption, excitation, emission and lifetime analysis of the samples have been carried out. Judd–Ofelt theory has been used to estimate several parameters for $DyCl_3$ and $Dy(Sal)_3Phen$ in PVA polymer film which show fair agreement between the experimental and the theoretical values supporting the J–O theory. A combination of blue and yellow emissions in $Dy_x(Sal)_3Phen$ co-doped PVA samples makes one perceive cool white light when excited by ultraviolet light. Energy transfer (ET) from Sal to Dy^{3+} is investigated by directly observing the luminescence intensity of Dy^{3+} in the $Dy_x(Sal)_3Phen$ co-doped PVA samples which is much stronger than that in the $DyCl_3$ in PVA which is further confirmed by lifetime studies with different concentrations of Dysprosium ion (Dy^{3+}). The generation of white light with chromaticity coordinates (0.30, 0.34) makes it potential material for white LED and display devices.

Keywords Energy transfer · Salicylic acid · Lanthanide complex · Photoluminescence · Judd–Ofelt theory · White light

PACs No. -95.75.Fg · 87.64.k- · 78.47.Jc · 64.70. Km · 33.50.-J · 68.35.bm

G. Kaur · S. B. Rai (✉)
Laser and Spectroscopy Laboratory, Department of Physics,
Banaras Hindu University,
Varanasi, India 221005
e-mail: sbrai49@yahoo.co.in

Introduction

White Light Emitting Diodes (LED)'s have received great attention in recent years due to their immense potential for the replacement of conventional incandescent and fluorescent lamps because they possess excellent properties such as high brightness, small volume, lower power consumption, high efficiency, long lifetime and the most important one is that they are environment friendly [1–4]. The phosphor powders used as white LED's employ two or three different phosphors or a full color display excited by UV light and those embedded in organic resin have poor heat-resistance [5–8]. Initiated by Zhang et al. [9], the rare earth (RE) doped glasses and glass ceramics emitting white light are receiving increasing interest in recent years overcoming the problems faced in conventional phosphors [10–13]. However, attempts are also being focused on exploiting RE doped polymers as light emitting diodes and biosensors etc. [14–17]. These also bear some potential advantages over glasses such as easy fabrication, molding into any shapes, homogeneous light splitting, efficient luminescence, non-toxicity, excellent heat-resistance and above all, cost effectiveness in every aspect. The critical aspect of using RE doped polymer systems is the non-feasibility of directly dispersing inorganic RE salts into an organic matrix and an attempt of direct inclusion of RE ions in the polymer usually results in an ionic aggregation. Also the emission efficiency of the RE strongly suffers due to the higher lattice vibrations of C–H (~3,000 cm^{-1}), O–H (~3,200 cm^{-1}) bonds etc. [18, 19]. To counter these problems, RE ions are encapsulated by organic ligands which act as an antenna ligand ions and transfer their absorbed energy to them. Many studies have inferred Salicylic acid (Sal) as one of such effective ligand which chelates as well as sensitizes

the RE ions and above all, it itself yields strong blue emission. Besides this, 1, 10-Phenanthroline was added to it for structural rigidity and reducing the rate of non-radiative decays [20, 21]. Poly Vinyl Alcohol (PVA) polymer exhibits good mechanical properties and susceptibility to biodegradation, and is widely used in industries, pharmaceuticals and medical fields [22]. Among all the lanthanide ions, Dy^{3+} ion gives most intense emission in yellow region for our purpose to achieve white light by intermixing of complementary blue and yellow colors [23–25].

Present work deals with synthesis of $DyCl_3$ and $Dy(Sal)_3Phen$ in PVA polymer films by solution casting technique. The spectroscopic properties of Dy^{3+} ion in PVA polymer in the absence and presence of Sal/Phen has been investigated. The Judd–Ofelt intensity parameters and other radiative properties are calculated which show improved absorption and emission cross-sections for Dy^{3+} ion in the presence of Sal. This enhancement is explained due to encapsulation effect and energy transfer from Salicylic acid to Dy^{3+} ions. The tunability to white emission by mixing of blue and yellow colors from the individual constituents is reported under UV excitation. Luminescence kinetics has also been examined using time resolved technique.

Materials

Dysprosium oxide (Dy) (99.95%), Salicylic acid (Sal) (99.9%), 1, 10-phenanthroline (Phen) (99.5%) and Poly vinyl Alcohol (PVA) (mw. 14000) have been purchased from Sigma Aldrich and were used without further purification. $DyCl_3$ (0.3 mol%) was obtained by dissolving Dy_2O_3 in concentrated HCl to which ethanolic solution of Salicylic acid (0.1 mol%) and 1, 10-phenanthroline (0.03 mol%) was added drop wise and stirred for half an hour. The detailed procedure to get $Dy(Sal)_3Phen$ complex has been given by Melby et al. [26] and the desired thin films were obtained according to the process given in our earlier work [26, 27]. Samples with different concentration of Dy^{3+} ion were prepared for luminescence measurements. The structure of the RE ion with Sal and Phen has been discussed by several groups indicating that both the carboxylic and the phenolic oxygen atoms coordinate with central RE ion with coordination number lying between 6 and 9 [28, 29].

The absorption spectra were recorded using a Cary 2390 double beam UV-Vis-NIR spectrophotometer in the wavelength region 300–1,350 nm. For excitation and emission spectra a Spectrofluorometer [Fluoromax-4, Horiba JobinYvon attached with a continuous source] and third harmonic (355 nm) of Nd:YAG laser [Spitlight-600, Innolas, Germany] respectively was used. Photoluminescence decay measurements were carried out using 355 nm pulsed laser radiation with pulse width 7 ns, as an excitation source. The collected signal was fed to a 150 MHz digital oscilloscope (model no. HM 1507, Hameg Instrument) to get the decay curve. Lifetime of the radiative levels was estimated by fitting the decay curves to exponential function. The detector offset was removed before fitting and the data were normalized to the initial voltage. Photographs of the sample were clicked with an ordinary camera with samples kept in a UV chamber.

Results and Discussion

Absorption Spectra and Judd–Ofelt Analysis

UV-Vis-NIR absorption spectra of $DyCl_3$ and $Dy(Sal)_3Phen$ in PVA films were recorded in the range of 300–1,350 nm under identical condition and depicted in Fig. 1. Absorption spectrum of $DyCl_3$ in PVA consists of weak absorption bands at 325, 349, 363, 385, 751, 800, 907, 1,093 and 1,290 nm that are assigned to electronic transitions from the $^6H_{15/2}$ (ground state) to different excited states viz. $^6P_{3/2}$, $^6P_{7/2}$, $^4D_{3/2} + {}^6P_{5/2}$, $^4K_{17/2} + {}^4F_{7/2}$, $^6F_{3/2}$, $^6F_{5/2}$, $^6F_{7/2} + {}^6H_{5/2}$, $^6F_{9/2} + {}^6H_{7/2}$ and $^6F_{11/2} + {}^6H_{9/2}$ respectively of Dy^{3+} ion. On adding Sal/Phen to it as in $Dy(Sal)_3Phen$ in PVA, the absorption intensity for the bands increase and two new peaks at 449 and 473 nm start appearing due to transitions from $^6H_{15/2}$ to $^4I_{15/2}$ and $^4F_{9/2}$ respectively.

In the lanthanide-organic coordinated systems, the encapsulation of RE (Dy^{3+}) ion with the organic ligand (Sal/Phen) shields it from the interaction with the host matrix (PVA), which effectively prevents the non-radiative recombination via matrix phonons. The decoupling of Dy^{3+} ion from the host improves the 4f-4f optical transition intensities, consequently responsible for increase in absorbance and appearance of new bands.

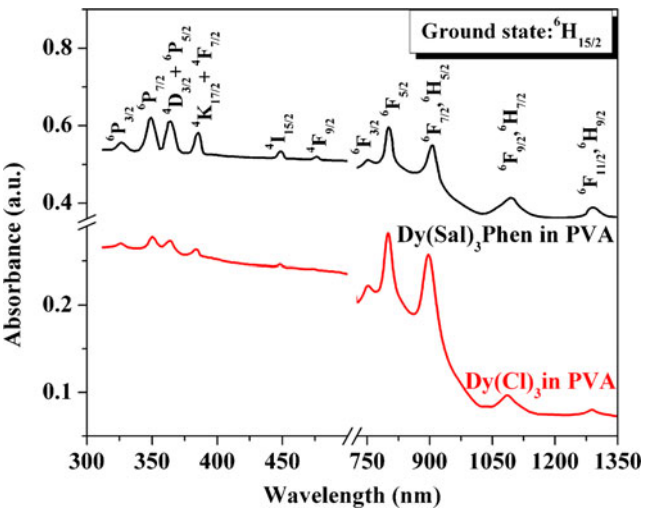

Fig. 1 UV-Vis-IR absorption spectra of $DyCl_3$ and $Dy(Sal)_3Phen$ in PVA films

Nephelauxetic Ratio and the Bonding Parameter

To have an idea about the nature of bond between Dy ion and associated ligand (Sal/Phen), the nephelauxetic ratios and bonding parameters have also been evaluated. The nephelauxetic ratio (β) is given by ν_c/ν_a, where ν_c is the wavenumber (in cm^{-1}) of a particular transition for an ion in the host under investigation and ν_a is the wavenumber (in cm^{-1}) of the same transition for the aquo ion. From the average value of β, (taken as β_{avg}) the bonding parameter (δ) could be calculated using an expression $\delta = 1 - \left(\beta/\beta_{avg}\right) \times 100$. The metal-ligand bond will be covalent or ionic depending upon the positive or negative sign of β and δ. The calculated nephelauxetic ratios (β) and the bonding parameters (δ) with the respective energies for different transitions from ground state $^6H_{15/2}$ in the polymer host and aquo ion are tabulated in Table 1. From the derived nephelauxetic ratios and bonding parameters, it is concluded that the bonding is of ionic character.

Judd–Ofelt Analysis

Judd–Ofelt theory is widely used for quantitative characterization of 4f-4f optical transitions in RE doped systems. According to Judd–Ofelt theory [30, 31] the calculated oscillator strength of an induced electric-dipole transition from the ground state ψ_J to an excited state $\psi'_{J'}$ is given by

$$f_{cal} = \frac{8\pi^2 mc\nu}{3h(2J+1)} \frac{\left(n^2+2\right)^2}{9n} \sum_{\lambda=2,4,6} \Omega_\lambda \left(\Psi J \left\| U^\lambda \right\| \Psi' J'\right)^2 \quad (1)$$

where n is the refractive index of medium, ν is the energy of transition in cm–1, $\frac{\left(n^2+2\right)^2}{9n}$ is the Lorentz local field correction, J is the total angular momentum of ground state and J′ that of the excited state, Ω_λ (λ=2, 4, 6) are J–O intensity parameters $\|U^{(\lambda)}\|^2$ are the doubly reduced matrix elements of the unit tensor operator evaluated under the approximation of intermediate coupling scheme for a transition ψ_J to $\psi'_{J'}$. The experimental oscillator strength (f_{exp}) of an absorption band is directly proportional to the area under the absorption curve and is expressed as

$$f_{exp} = \frac{2.303mc^2}{N_A \pi e^2} \int \varepsilon(\nu) d\nu = 4.318 \times 10^{-9} \int \varepsilon(\nu) d\nu \quad (2)$$

where m and e are the mass and charge of electron, c is the velocity of light, N_A is the Avogadro's number, and ε (ν) is the molar absorptivity of the transition at frequency ν (cm^{-1}). A comparison of calculated and experimental oscillator strength for Dy^{3+} ions in the presence and absence of Sal/Phen is given in Table 2.

A measure of accuracy of the fit between the experimental and calculated oscillator strengths is given by the root mean square (rms) deviation

$$\sigma_{rms} = \left[\frac{\sum \left(f_{exp} - f_{cal}\right)^2}{N}\right]^{1/2} \quad (3)$$

where N is the number of levels included in the fit. The small rms deviation indicates a better fit between the experimental and theoretical oscillator strengths.

A least square fit method is then used for Eq. 1 to determine Ω_λ (λ=2, 4 and 6) parameters, which gives the best fit to the experimental values. The calculated oscillator strengths (f_{cal}) are obtained using Eq. 1 and the phenomenological parameters Ω_λ, which in turn form the basis for the calculation of other spectroscopic properties such as radiative transition probability, branching ratio, radiative lifetime, etc.

Table 1 The nephelauxetic ratio (β) and the bonding parameter (δ) for $Dy(Sal)_3$ PVA film with respective energies for different transitions from ground state $^6H_{15/2}$ in the host and aquo ion

Transitions from level $^6H_{15/2}$	$Dy(Sal)_3$ in PVA				
	Wavelength (nm)	Energy(ν_c) (cm^{-1})	Energy aquo (ν_a)[a] (cm^{-1})	NFE ratio (β)	(δ)
$^6F_{11/2} + {}^6H_{9/2}$	1,290	7,752	7,700	1.0068	−0.119
$^6F_{9/2} + {}^6H_{7/2}$	1,093	9,149	9,100	1.0054	−0.020
$^6F_{7/2} + {}^6H_{5/2}$	907	11,025	11,000	1.0023	−0.328
$^6F_{5/2}$	800	12,500	12,400	1.0081	−0.218
$^6F_{3/2}$	751	13,316	13,250	1.0049	−0.069
$^4F_{9/2}$	473	21,141	21,100	1.0019	−0.368
$^4I_{15/2}$	449	22,271	22,100	1.0071	−0.208
$^6K_{17/2} + {}^4F_{7/2}$	385	25,974	25,800	1.0067	−0.109
$^4D_{3/2} + {}^6P_{5/2}$	363	27,548	27,400	1.0054	−0.020
$^6P_{7/2}$	349	28,653	28,550	1.0036	−0.198
$^4P_{3/2}$	325	30,769	30,500	1.0088	−0.318
				β_{avg}=1.0056	

[a]The values of the energies of respective transitions in aquo ion have been taken from ref. [23]

Table 2 A comparison of experimental and calculated oscillator strengths ($\times 10^{-6}$) in $DyCl_3$ and $Dy(Sal)_3$ in PVA films

Transitions from level $^6H_{15/2}$	$DyCl_3$ in PVA		$Dy(Sal)_3$ in PVA	
	Experimental	Calculated	Experimental	Calculated
$^6F_{11/2} + {}^6H_{9/2}$	2.984	2.991	3.001	3.121
$^6F_{9/2} + {}^6H_{7/2}$	2.691	2.708	2.814	2.304
$^6F_{7/2} + {}^6H_{5/2}$	2.432	2.218	2.780	2.740
$^6F_{5/2}$	1.143	1.134	1.297	1.469
$^6F_{3/2}$	0.213	0.199	0.579	0.680
$^4F_{9/2}$	–	–	0.090	0.081
$^4I_{15/2}$	–	–	0.121	0.119
$^6K_{17/2} + {}^4F_{7/2}$	1.443	1.780	1.982	1.891
$^4D_{3/2} + {}^6P_{5/2}$	1.063	1.103	1.379	1.471
$^6P_{7/2}$	2.767	2.756	3.001	2.998
$^4P_{3/2}$	0.845	0.900	1.020	0.939
	N=9		N=11	
	$\sigma = \pm 0.18 \times 10^{-6}$		$\sigma = \pm 0.24 \times 10^{-6}$	

It is possible to predict the microenvironment and the bonding parameters in the vicinity of the RE ion with the knowledge of J–O intensity parameters [31]. The parameter Ω_2 is associated to the symmetry of the ligand field, and is sensitive to the structural changes in the RE site. The parameters Ω_4 and Ω_6 are dependent on the bulk properties of the material viz. viscosity and dielectric constant of the media and are influenced by the vibronic transitions of the RE ions bonded to the ligand [32]. Judd–Ofelt parameters which have not yet been reported for polymer systems have been calculated for $DyCl_3$ and $Dy(Sal)_3Phen$ in PVA film and compared with Ω_λ values for Dy^{3+} ion in other hosts in Table 3. The trend of the J–O parameters in $DyCl_3$ PVA film is $\Omega_2 > \Omega_4 = \Omega_6$ while it follows the trend as $\Omega_2 > \Omega_4 > \Omega_6$ in case of $Dy(Sal)_3Phen$ in PVA film. It is obvious from the table that the value of Ω_2 parameter for $DyCl_3$ PVA sample is lower than the value of $Dy(Sal)_3Phen$ PVA sample, which is a result of higher covalent bonding and higher asymmetry [33]. A Dy^{3+} ion is coordinated by three Salicylate and a Phen ligand which form a sheath around the central Dy^{3+} ion, protecting it from high frequency vibrations of the host and the ion-ion interactions, facilitating the higher RE ion doping without quenching effect.

Radiative Properties

The J–O parameters have been used to predict various important radiative parameters viz. radiative transition probability (A), branching ratio (β_R), effective band width ($\Delta\lambda_{eff}$) and stimulated emission cross-section ($\sigma(\lambda_p)$) for a particular transition of RE ion. Different radiative properties for a particular transition have been calculated for $DyCl_3$ and $Dy(Sal)_3Phen$ in PVA samples and tabulated in Table 4. It is clear from the table that the experimental (β_R) values are in close agreement with the predicted values using the JO theory. Also, the radiative properties of Dy^{3+} ion enhance in the presence of Sal/Phen ligand in PVA film.

Excitation Spectra

The excitation spectra of $DyCl_3$ and $Dy(Sal)_3Phen$ in PVA films corresponding to $^4F_{9/2} \rightarrow {}^6H_{13/2}$ (572 nm) transition in the region 275–450 nm are shown in Fig. 2. Several excitation bands are observed in $DyCl_3$:PVA and these are assigned as electronic transitions from ground level $^6H_{15/2}$ to higher energy levels of Dy^{3+} ions i.e. $^6H_{15/2} \rightarrow {}^4H_{11/2}$ (294 nm), $^6H_{15/2} \rightarrow {}^6P_{3/2}$ (325 nm), $^6H_{15/2} \rightarrow ({}^4M, {}^4I)_{15/2}$, $^6P_{7/2}$

Table 3 A comparison of J–O intensity parameters ($\times 10^{-20}$) cm^2 for $DyCl_3$ and $Dy(Sal)_3$ in PVA films with other hosts

Sample	Ω_2	Ω_4	Ω_6	Ω_4/Ω_6	Trend	Reference
$DyCl_3$ in PVA	3.670	1.939	1.939	1.00	$\Omega_2>\Omega_4=\Omega_6$	This work
$Dy(Sal)_3$ in PVA	5.978	4.333	2.679	1.61	$\Omega_2>\Omega_4>\Omega_6$	This work
Tellurite Glass	5.19	1.93	1.07	1.80	$\Omega_2>\Omega_4>\Omega_6$	[11]
Calcium Fluoroborate Glass	5.98	2.33	2.33	1.00	$\Omega_2>\Omega_4=\Omega_6$	[23]
Barium Fluoroborate Glass	2.90	1.09	0.97	1.12	$\Omega_2>\Omega_4>\Omega_6$	[36]
Borate Glass	4.90	0.94	2.07	0.45	$\Omega_2>\Omega_4<\Omega_6$	[38]

Table 4 Calculated radiative parameters viz. radiative transition probability (A in (s^{-1})), branching ratio (β_R) (experimental and calculated), effective band width ($\Delta\lambda_{eff}$) and stimulated emission cross-section ($\sigma(\lambda_p)$ in ($\times 10^{-22}$ cm^2)) for $DyCl_3$ and $Dy(Sal)_3$ in PVA films

Transitions (Energy cm^{-1})	$DyCl_3$ in PVA					$Dy(Sal)_3$ in PVA				
	A	(β_R)		$\Delta\lambda_{eff}$	$\sigma(\lambda_p)$	A	(β_R)		$\Delta\lambda_{eff}$	$\sigma(\lambda_p)$
	(s^{-1})	exp.	cal.		$\times 10^{-22}$ cm^2	(s^{-1})	exp.	cal.		$\times 10^{-22}$ cm^2
$^4F_{9/2}\rightarrow{}^6H_{15/2}$ (~20,747)	175	0.182	0.158	15.42	0.31	201	0.230	0.181	17.03	0.34
$^4F_{9/2}\rightarrow{}^6H_{13/2}$ (~17,482)	686	0.721	0.689	13.94	2.83	724	0.746	0.734	14.76	2.98
$^4F_{9/2}\rightarrow{}^6H_{11/2}$ (~15,083)	70	0.059	0.045	14.61	0.36	79	0.064	0.069	14.92	0.45
$^4F_{9/2}\rightarrow{}^6H_{9/2}$ (~13,315)	59	0.051	0.059	16.23	0.34	71	0.057	0.061	16.45	0.37
$^4F_{9/2}\rightarrow{}^6H_{7/2}$ (~11,990)	18	0.019	0.021	15.59	0.29	26	0.020	0.018	16.80	0.36

(349 nm), $^6H_{15/2}\rightarrow{}^6P_{5/2}$, $^4I_{11/2}$ (363 nm), $^6H_{15/2}\rightarrow{}^4I_{13/2}$, $^4F_{7/2}$ (386 nm), and $^6H_{15/2}\rightarrow{}^4G_{11/2}$ (425 nm). A similar pattern of excitation bands of Dy^{3+} ion appears in $Dy(Sal)_3Phen$ in PVA except an enhancement in the intensity due to encapsulation and a broad excitation band in the range of 335–370 nm in $Dy(Sal)_3Phen$ doped PVA film. Appearance of this band signifies that the organic ligand (Sal/Phen) is within coordination sphere of Dy^{3+} ions, hence efficiently absorbing the excitation energy (355 nm) and transferring to Dy^{3+} ions and hence Sal/Phen acts as "antenna ligand" for Dy^{3+} ions.

Photoluminescence Spectra on 355 nm Excitation

The photoluminescence spectra of $DyCl_3$ and $Dy(Sal)_3Phen$ in PVA excited by 355 nm radiation are shown in Fig. 3. The spectra of $DyCl_3$ in PVA contains two intense bands, one in blue (481 nm) and the other in yellow (572 nm) region and two weak bands in red (663 and 751 nm) regions which are attributed to transitions from $^4F_{9/2}$ to ^6H_J (J=15/2, 13/2, 11/2 and 9/2). Among them yellow band is the most intense. In case of $Dy(Sal)_3Phen$ in PVA, there appears a broad band stretching from 375 to 475 nm for Sal and an increase in intensity for the peaks due to Dy^{3+}. Also, it is worthwhile to mention the appearance of a new peak at 834 nm for transition from $^4F_{9/2}$ to $^6H_{7/2}$ in Dy^{3+} ion which is rarely observed. In the present situation, we report ~4 times enhancement in emission intensity ratio as we go from $DyCl_3$ to $Dy(Sal)_3Phen$ doped in PVA. The enhancement of the fluorescence is probably due to the encapsulation effect of RE ions as stated in case of absorption and also attributed to energy transfer process from Sal to Dy^{3+} ions [34].

The mechanism involved is explained as: The 355 nm radiation excites Dy^{3+} ions to the $^6P_{3/2}$ level. The Dy^{3+} ion from there relax non-radiatively due to higher phonon frequency (~1,300 cm^{-1}) and finally populate the long lived

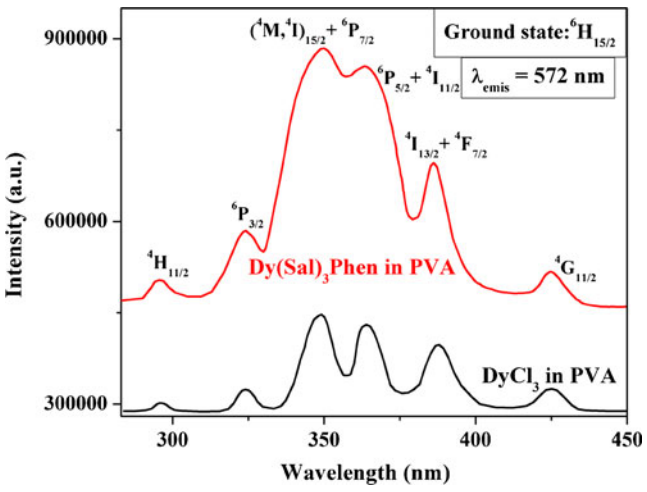

Fig. 2 Excitation spectra of $DyCl_3$ and $Dy(Sal)_3Phen$ in PVA films corresponding to 572 nm emission ($^4F_{9/2}\rightarrow{}^6H_{15/2}$ transition) of Dy^{3+} ion. An additional broad band (340–360 nm) appears due to the sensitization of Sal for Dy^{3+} ions

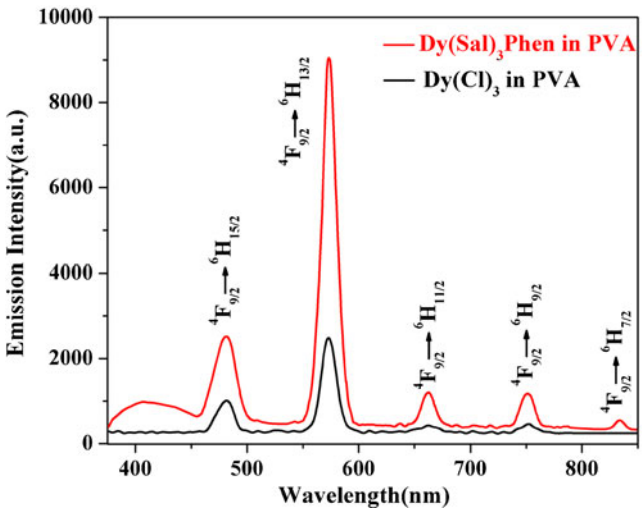

Fig. 3 Photoluminescence spectra of $DyCl_3$ and $Dy(Sal)_3Phen$ in PVA films under 355 nm excitation

$^4F_{9/2}$ level (~550 μs). The $^4F_{9/2}$ level gives radiative transition to the ground state ^6H_J (J=15/2, 13/2, 11/2 9/2 and 7/2 levels) respectively.

The organic carboxylate ligands adopt several coordination modes to form polynuclear complexes viz. bridging mode and bridging-chelating mode. However, for the efficient energy transfer from any organic species to RE ion, two essential conditions are to be satisfied. First: the excited level of the RE ion should be lower than the lowest triplet state of the organic compound, and the second: the lifetime of the triplet level should neither be too short to achieve an energy transfer nor too long to effectively populate the excited level [14, 19, 35]. Moreover the direct coordination of the Sal to Dy^{3+} ion improves the energy-transfer efficiency due to reduced donor-acceptor distance. The mechanism involved in the photoluminescence enhancement of Dy^{3+} ions by Sal in PVA is understood in the light of these facts. The 355 nm laser photon excites Sal to its singlet state (S_1). An excited state intramolecular proton transfer process from the –OH group to the C=O group of Sal takes place. Furthermore it's dimeric and the tautomeric form emits energy in blue region (~410 nm) which acts as antenna ligand for RE (Dy^{3+}) ions [21, 27, 33]. A part of the energy of Sal is also lost through intersystem crossing to triplet state (T_1), which is then transferred to the chelated Dy ion. The lowest triplet state of Sal lies at 24,184 cm^{-1} [36] which infact is in resonance with $^4G_{11/2}$ level of Dy^{3+} and transfers its energy easily to Dy^{3+} ions. The $^4F_{9/2}$ level populated through non-radiative process gives radiative emissions to different levels of ground state. Schematic energy level diagram for Dy^{3+} ion and Salicylate anion alongwith the possible pathways for energy transfer to Dy^{3+} ion is illustrated in Fig. 4.

Further, by increasing the concentration of Sal, the emission of Dy^{3+} ion increases while by increasing the concentration of Dy^{3+} ions the emission intensity of Sal band reduces monotonically, which supports the energy transfer mechanism. The intra-molecular energy transfer efficiency calculated is 61% [see ref. 37]. The relative quantum yield of $DyCl_3$ and $Dy(Sal)_3Phen$ is calculated by comparing the emission intensity with the emission intensity of Coumarin 540 dye. The measured quantum yields were found to be 4.2% and 12.11% for $DyCl_3$ and $Dy(Sal)_3Phen$ respectively. The higher emission intensity observed in $Dy(Sal)_3Phen$ in PVA film is due to transfer of absorbed energy of Sal to Dy^{3+} ions. Fluorescence emission from the $DyCl_3$ in PVA sample appears as yellow (see Fig. 5). The integrated intensity ratio between yellow and the blue bands have been found to be 2.7:1. The transition $^4F_{9/2}$ to $^6H_{13/2}$ is hypersensitive ($\Delta J=2$ and $\Delta L=2$) and its intensity is strongly influenced by the surrounding environment of the Dy^{3+} ion. A larger yellow to blue ratio confirms the higher degree of covalency between Dy^{3+} ion and O^{2-} ion [37] which is well in agreement with the J–O intensity parameters.

White Emission in $Dy_x(Sal)_3$ PVA Sample on 355 nm Excitation

The emission spectra of Sal in PVA and $Dy_x(Sal)_3Phen$ in PVA films were recorded in the range between 375 and 750 nm on excitation with 355 nm and are shown in Fig. 5. The concentration of Dy was varied from x=0 to 1.5 mol%. Sal doped PVA film yields a broad emission centered at 410 nm. Adding 0.3 mol% Dy^{3+} ions to it, three emission bands centered at 481, 572 and 663 nm assigned to $^4F_{9/2}\rightarrow{}^6H_{15/2}$, $^6H_{13/2}$ and $^6H_{11/2}$ transitions of Dy^{3+} ions respectively are seen alongwith decrease in intensity of Sal emission. On increasing the concentration of Dy^{3+} ions further (from 0.3 to 1.2 mol%) in the PVA sample, there is a regular decrease in Sal emission and increase in intensity of Dy^{3+} peaks. The variation of Sal emission at 410 nm and yellow emission of

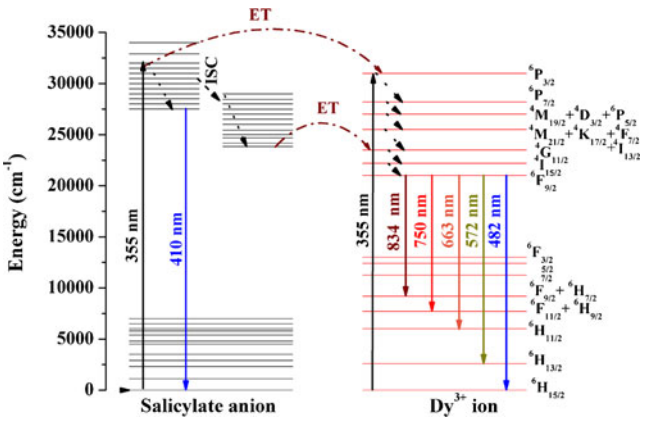

Fig. 4 Schematic energy level diagram for Dy^{3+} ion and Salicylate anion. The possible pathways for sensitization by Sal anion and energy transfer to Dy^{3+} ion is illustrated. The radiative transitions are represented by *solid lines* and the non-radiative ones by *dotted lines*

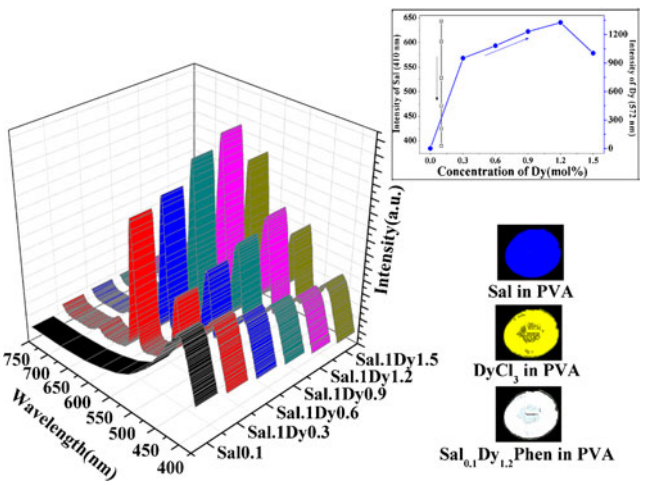

Fig. 5 Luminescence spectra of $Dy(Sal)_3Phen$ doped PVA film under 355 nm excitation

Dy^{3+} ions at 572 nm with respect of the concentration of Dy^{3+} ions is shown in inset to Fig. 5. A further increase in concentration of Dy (1.5 mol%) quenches the emission intensity due to energy migration among Dy–Dy ions [38].

The color of luminescence can be altered from blue to cool bluish white by properly adjusting the intensity of complementary yellow color from Dy^{3+} ions which is made possible by varying the concentration of Dy^{3+} ions. This adjustability of luminescence color also broadens the application areas. The Commission Internationale de Eclairage (CIE) chromaticity coordinates for $Dy_x(Sal)_{0.1}Phen$(x=0, 0.3, 0.6, 0.9, 1.2 and 1.5) PVA are calculated based on the corresponding emission spectra and are presented in Fig. 6. The sample with the respective concentrations of Sal and Dy as $Sal_{0.1}Dy_{0.0}$ shows blue emission from Sal with CIE coordinates as (X=0.17, Y=0.02). On adding 0.3 mol% Dy to it, the coordinates change to (X=0.25, Y=0.25) and further enhancing the concentration of Dy to 1.2 mol%, the sample starts appearing bluish white (cool white) with coordinates (X=0.30, Y=0.34) which is close to the normal white light (0.333, 0.333). The photographs of the samples are shown in the inset to Fig. 5. Thus, we can infer that white light can be synthesized by proper combinations of blue and yellow light by appropriately tuning the ratios of Dy^{3+} and Sal in PVA polymer under UV excitation.

Time-Resolved Photoluminescence Spectroscopy

The energy transfer from Sal to Dy^{3+} ion could be verified with the time resolved photoluminescence studies of $^4F_{9/2}\rightarrow{}^6H_{13/2}$ (572 nm) transition of Dy^{3+} ion with 355 nm excitation. The observed luminescence decay curves are depicted in Fig. 7. The measured lifetime (τ_{meas}) of $^4F_{9/2}$ fluorescent level has been determined by taking first e-folding time of the decay curve. In case of $DyCl_3$ doped PVA film, the lifetime estimated is ~562 μs. On the other hand the, decay curves of PVA film doped with $Dy_x(Sal)_3Phen$ where x=0.3, 0.6 and 1.2 mol% of Dy^{3+} give the values of lifetime as ~653 μs which further reduces to ~587 μs on increasing the concentration of Dy^{3+} ions. Firstly the increase in lifetime of Dy^{3+} ion on addition of Sal is attributed to the efficient feedback from Sal (~ms) which enhances the population density of fluorescent level of Dy^{3+} ion and also due to the shielding of Dy^{3+} ion from the –CH and –OH vibrations of host which are responsible for non-radiative processes and decrementing the lifetime. Further dipole-dipole interactions begin to prevail between two proximate Dy^{3+} ions as the concentration increases and thus, reduction in lifetime is observed which shows the involvement of non-radiative processes. Due to the favorable energy matching condition, a resonant energy transfer is possible implying the energy releasing through excited Dy^{3+} ion to unexcited Dy^{3+} ion which decreases the lifetime and quenches the emission intensity. Also there may be the occurrence of cross-relaxation process [39].

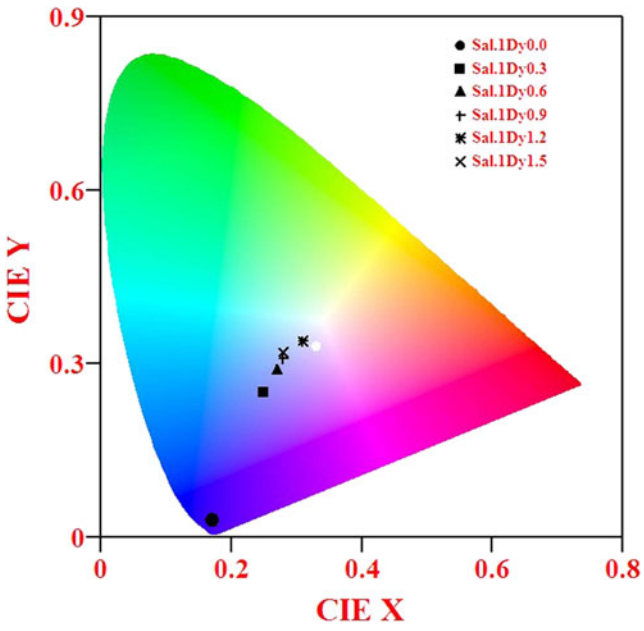

Fig. 6 Commission Internationale de Eclairage (CIE) chromaticity coordinates for $Dy_x(Sal)_3Phen$ in PVA film where x varies from 0 to 1.5 mol%

Conclusions

A comparative study of optical properties of $DyCl_3$ and $Dy(Sal)_3Phen$ in PVA polymer film have been made. The nephelauxetic ratios, bonding parameters and several different radiative properties for Dy ions have been calculated in polymer host, which shows reasonable agreement between

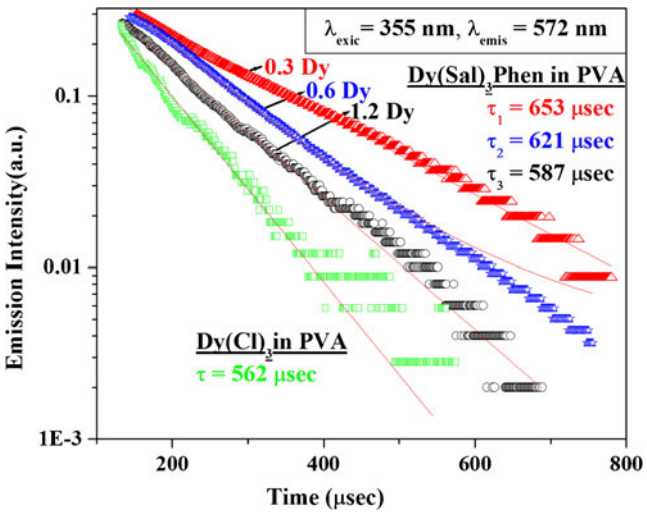

Fig. 7 Decay curves of $^4F_{9/2}\rightarrow{}^6H_{13/2}$ (572 nm) transition of Dy^{3+} ion in $DyCl_3$ and $Dy_x(Sal)_3Phen$ in PVA film where x=0.3, 0.6 and 1.2

the experimental and the theoretical values supporting the J–O theory. It was also observed that the radiative properties of Dy^{3+} ion in $Dy(Sal)_3Phen$ improves due to the encapsulation and also due to energy transfer from Sal to Dy^{3+} ions. Intense yellow and blue emissions were visualized under 355 nm excitations for $DyCl_3$ and Sal in PVA respectively which can be tuned to white light with coordinates (0.30, 0.34) by adjusting the ratios of the two. The results indicate that $Dy(Sal)_3Phen$ in PVA is potential material for white light-emitting diodes (LEDs).

Acknowledgements Authors are grateful to the AvH foundation, Germany for providing pulsed Nd:YAG laser. One of the authors (G. Kaur) would like to thanks CSIR (India) for Senior Research Fellowship.

References

1. Zeuner M, Hintze F, Schnick W (2009) Low temperature precursor route for highly efficient spherically shaped LED-PHOSPHORS $M_2Si_5N_8:Eu^{2+}$ (M = Eu, Sr, Ba). Chem Mater 21:336–342
2. Allen SC, Steckl AJ (2008) A nearly ideal phosphor-converted white light-emitting diode. Appl Phys Lett 92:143309–143311
3. Song X, Fu R, Agathopoulos S, He H, Zhao X, Yu X (2011) Synthesis of BaSi2O2N2:Ce3+, Eu2+ phosphors and determination of their luminescence properties. J Am Ceram Soc 94:501–507
4. Schubert EF, Kim JK (2005) Solid-state light sources getting smart. Science 308:1274–1278
5. Yanna X, Fen X, Qinyan Z, Zhonghong J (2009) Synthesis and luminescent properties of poly crystalline Gd2(MoO)4:Dy3+ for white light emitting diodes. J Rare Earths 27:753–757
6. Xie RJ, Hirosaki N, Mitomo M, Takahashi K, Sakuma K (2006) Highly efficient white-light-emitting diodes fabricated with short-wavelength yellow oxynitride phosphors. Appl Phys Lett 88:101104–101107
7. Kim JS, Lim KT, Jeong YS, Jeon PE, Choi JC, Park HL (2005) Full-color $Ba_3MgSi_2O_8:Eu^{2+}$, Mn^{2+} phosphors for white-light-emitting diodes. Solid State Commun 135:21–24
8. Nishiura T, Tanabe S (2009) Preparation and luminescence properties of glass ceramics precipitated with {MMgSiO :Eu}(M = Sr, Ca) phosphor for white light source. IEEE J Sel Top Quantum Electron 15:1177–1180
9. Zhang JC, Parent C, le Flern G, Hagenmuller P (1991) White light emitting glasses. J Solid State Chem 93:17–29
10. Cui R, Ye Z, Hua Y, Deng D, Zhao S, Li C, Xu S (2011) Eu2+/Dy3+ co-doped white light emission glass ceramics under UV light excitation. J Non-Crystalline Solids 357:2282–2285
11. Babu AM, Jamalaiah BC, Kumar JS, Sasikala T, Moorthy LR (2011) Spectroscopic and photoluminescence properties of Dy3+ −doped lead tungsten tellurite glasses for laser materials. J Alloy Compd 509:457–462
12. Liu S, Zhao GL, Ying H, Wang JX, Han GR (2008) Eu/Dy ions co-doped white light luminescence zinc–aluminoborosilicate glasses for white LED. Opt Mater 31:47–50
13. Lakshminarayana G, Yang R, Qiu JR, Brik MG, Kumar GA, Kityk IV (2009) White light emission from Sm3+/Tb3+ codoped oxyfluoride aluminosilicate glasses under UV light excitation. J Phys Appl Phys 42:015414–015426
14. Binnemans K (2005) Handbook on the Physics and Chemistry of Rare Earths Ch 225 edited by K.A. Gschneidner, Jr., J.-C.G. Bünzli and V.K. Pecharsky, 35:111–272
15. Hebbink G (2002) Ph. D Thesis, Twente University Press, Netherlands
16. Kaur G, Rai SB (2011) J Phys D: Appl Phys (Accepted)
17. Elashmawi IS, Hakeem NA, Selim MS (2009) Optimization and spectroscopic studies of CdS/poly(vinyl alcohol) nanocomposites. Mater Chem Phys 115:132–135
18. Okamoto Y, Ueba Y, Dzhanibekov NF, Banks E (1981) Rare earth metal containing polymers. 3. Characterization of ion-containing polymer structures using rare earth metal fluorescence probes. Macromolecules 14:17–22
19. Nagato I, Li R, Banks E, Okamoto Y (1983) Energy transfer from donor to acceptor ions in perfluorosulfonate membraned. Macromolecules 16:903–905
20. Binnemans K (2009) Lanthanide-based luminescent hybrid materials. Chem Rev 109:4283–4374
21. Bisht PB, Tripathi HB, Pant DD (1995) Cryogenic studies, site selectivity and discrete fluorescence in salicylic acid dimer. J Photochem Photobiol Chem 90:103–108
22. Kumar GNH, Rao JL, Gopal NO, Narasimhulu KV, Chakradhar RPS, Rajulu AV (2004) Spectroscopic investigations of Mn2+ ions doped Polyvinylalcohol films. Polymer 45:5407–5415
23. Kumar JS, Pavani K, Babu AM, Giri NK, Rai SB, Moorthy LR (2010) Fluorescence characteristics ofDy3+ ions in calcium fluoroborate glasses. J Lumin 130:1916–1923
24. Hu X, Fan J, Pan J, Gao J, Li T, Zhang D, Zheng X, Jiang D, Liu E (2009) The blue-light emission enhancement mechanism of Eu2+ in Eu, Dy: SiO2 matrix. Opt Mater 31:1707–1710
25. Rayappan IA, Marimuthu K, Babu SS, Sivaraman M (2010) Concentration dependent structural, optical and thermal investigations of Dy3+− doped sodium fluoroborate glasses. J Lumin 130:2407–2412
26. Melby LR, Rose NJ, Abramson E, Caris JC (1964) Synthesis and fluorescence of some trivalent lanthanide complexes. J Am Chem Soc 86:5117–5125
27. Kaur G, Dwivedi Y, Rai SB (2011) Gd^{3+} sensitized enhanced green luminescence in $Gd:Tb(Sal)_3Phen$ complex in PVA. J Fluoresc 21:423–432
28. Burns JH, Baldwin EH (1977) Crystal structures of aquotris (salicylato)samarium(III) and aquotris (salicylato)americium(III). Inorg Chem 16:289–294
29. Durham DA, Hart FA (1969) Lanthanide complexes—VI. Complexes of yttrium and lanthanide thiocyanates, chlorides, nitrates and salicylates with 1,2-bis(pyridine-α-aldimino)ethane. J Inorg Nucl Chem 31:145–157
30. Judd BR (1962) Optical absorption intensities of rare-earth ions. Phys Rev 127:750–761
31. Ofelt GS (1962) Structure of the f6 configuration with application to rare-earth ions. J Chem Phys 49:511–520
32. Tanabe S, Ohayagi T, Soga N, Hanada T (1992) Compositional dependence of Judd–Ofelt parameters of Er^{3+} ions in alkali-metal borate glasses. Phys Rev 46:3305–3310
33. Kaur G, Dwivedi Y, Rai SB (2010) Study of enhanced red emission from $Sm(Sal)_3Phen$ ternary complexes in Poly Vinyl Alcohol film. Opt Commun 283:3441–3447
34. Cunjin X (2006) Luminescent and thermal properties of Sm^{3+} complex with salicylate and o-phenanthroline incorporated in silica matrix. J Rare Earths 24:429–433
35. Elbanowski M, Makowska B (1996) The lanthanides as luminescent probes in investigations of biochemical systems. J Photochem Photobiol 99(2–3):85–92

36. Yan B, Zhang HJ, Wang SB, Ni JZ (1998) Intramolecular. Energy transfer mechanism between ligands internary complexes with aromatic acids and 1,10-phenanthroline. J Photochem Photobiol Chem 116:209–214
37. Dwivedi Y, Rai SB (2009) Spectroscopic study of Dy3+ and Dy3+/Yb3+ ions co-doped in barium fluoroborate glass. Opt Mater 31:1472–1477
38. Honma T, Toda K, Ye ZG, Sato M (1998) Concentration quenching of the Eu3+ activated luminescence in some layered perovskites with two dimensional arrangement. J Phys Chem Solids 59:1187–1193
39. Pisarska J (2009) Optical properties of lead borate glasses containing Dy3+ ions. J Phys Condens Matter 21:285101–285107